J Membrane Biol (2009) 227:123–131
DOI 10.1007/s00232-008-9151-3

Viewing the Bilayer Hydrocarbon Core Using Neutron Diffraction

Xue Han · Kalina Hristova

Received: 13 November 2008 / Accepted: 19 December 2008 / Published online: 24 January 2009

Abstract Membrane proteins fold, assemble and function within their native fluid lipid environment. Structural studies of fluid lipid bilayers are thus critically important for understanding processes in membranes. Here, we propose a simple approach to visualize the hydrocarbon core using neutron diffraction and deuterated lipids that are commercially available. This method should have broad utility in structural studies of the bilayer response to protein insertion and folding in membranes.

Keywords Membrane structure · Membrane biophysics · Biophysical techniques in membrane research

Introduction

Membrane proteins require a lipid environment for their folding, assembly and activity (White et al. 1998, 2001; White and Wimley 1999; Mackenzie 2006). The structure of the lipid bilayer is an important determinant of the structure, and hence the function, of the embedded membrane proteins; thus, many studies have been aimed at structural characterization of fluid bilayers (Nagle and Tristram-Nagle 2001; Wiener et al. 1989; Gandhavadi et al. 2002). Furthermore, the bilayer plays an active role during the processes of folding, insertion and translocation of proteins; therefore, studies have also focused on the effect of the embedded proteins on bilayer structure (Hristova et al. 1999; Hristova et al. 2001; Heller et al. 2000; Harroun et al. 1999). Structural studies of fluid bilayers, however, are challenging due to the very high thermal disorder that is intrinsic to the native membrane state (Wiener and White 1991a). This thermal disorder challenges the traditional views of structure and requires novel approaches for structural determination.

One of the popular bilayer structural characterization methods is diffraction of multilayers, which gives the transbilayer scattering density distribution (Heller et al. 2000; Nagle and Wiener 1988; Katsaras et al. 1991). More than 15 years ago White and colleagues proposed that since atomic positions in fluid bilayers cannot be resolved, diffraction experiments can be used to obtain the transbilayer distributions of different lipid structural groups, such as carbonyls, phosphate, choline, etc. (Wiener and White 1991b), and showed experimentally that these distributions are well described by gaussians (Wiener and White 1991c; Wiener et al. 1991). Based on this concept, Wiener and White (1992) then determined the complete structure of the DOPC bilayer at 66% relative humidity (RH), as given by the full set of such distributions.

Solving complete bilayer structures is a labor-intensive and time-consuming task, requiring acquisition of both X-ray and neutron data and utilizing multiple specifically labeled lipid analogues (Wiener and White 1992). Thus, 15 years after the accomplishment of Wiener and White, the DOPC structure at 66% RH remains the only complete bilayer structure that has been solved. Questions therefore arise as to how the complete structures of other bilayers compare to the DOPC structure at 66% RH and how the incorporation of proteins will alter these structures. Since it is not feasible to determine complete bilayer structures for every incorporated protein of interest, an alternative approach is to monitor the effect of peptide incorporation on the distribution of a particular lipid moiety. For

X. Han · K. Hristova (✉)
Department of Materials Science and Engineering,
Johns Hopkins University, Baltimore, MD 21218, USA
e-mail: kh@jhu.edu

instance, the effect of hydration and peptide incorporation on the hydrocarbon core (HC) has been studied by monitoring the changes in the transbilayer distribution of the double bonds in X-ray experiments (Hristova et al. 1999, 2001; Hristova and White 1998). This approach, however, requires bromine atom derivatization of the double bonds, and in some cases the bulky bromine atoms can perturb the bilayer structure (as we have observed for DOPC bilayers with 4 mole% melittin, unpublished results).

Here, we propose a different approach to monitor changes in the HC using neutron diffraction and deuterated lipids that are commercially available. The lipid we use is 1-palmitoyl (D31)-2-oleoyl-*sn*-glycero-3-phosphocholine, a POPC derivative with the palmitoyl chain deuterated. The comparison of scattering profiles of POPC bilayers with different concentrations of the deuterated POPC analogue allows straightforward determination of the HC distribution via contrast variation and easy calculation of the HC thickness. We demonstrate the feasibility of this approach for pure POPC bilayers, and we also determine the HC distribution in the presence of a peptide corresponding to the sequence of the TM domain of a human receptor tyrosine kinase.

Materials and Methods

Sample Preparation

1-Palmitoyl-2-oleoyl-*sn*-glycero-3-phosphocholine (POPC) and 1-palmitoyl (D31)-2-oleoyl-*sn*-glycero-3-phosphocholine ($POPC^D$, with the palmitoyl chain deuterated) were purchased from Avanti Polar Lipids (Alabaster, AL), and D_2O was obtained from Cambridge Isotope (Andover, MA). The peptide corresponding to the FGFR3 TM domain sequence, *RRAGSVYAGILSYGV GFFLFILVVAAVTLCRLR*, was synthesized as reported previously (Iwamoto et al. 2005). Four multilayer POPC/$POPC^D$ samples and two multilayer POPC/$POPC^D$ samples containing peptides were prepared and characterized using neutron diffraction. The four lipid multilayer samples were (1) 100 mole% POPC, (2) 95 mole% POPC + 5 mole% $POPC^D$, (3) 90 mole% POPC + 10 mole% $POPC^D$ and (4) 80 mole% POPC + 20 mole% $POPC^D$. The two lipid/peptide samples were (1) 96 mole% POPC + 4 mole% FGFR3 TM domain and (2) 96 mole% lipid (80 mole% POPC and 20 mole% $POPC^D$) + 4 mole% FGFR3 TM domain. The pure lipid multilayers were prepared by mixing POPC and $POPC^D$ in chloroform. The lipid/peptide samples were prepared by dissolving the peptides in a mixture of trifluoroethanol and hexafluoroisopropanol (1:2 ratio) and the lipids in chloroform (Li and Hristova 2004; You et al. 2005). The organic solutions were mixed in the appropriate ratios and deposited dropwise on a thin glass slide. The organic solvents were evaporated, and the samples were hydrated as described below. The size of each multilayer sample was about 15 mm × 17 mm × 5 μm.

Neutron Diffraction Experiments, Data Collection and Analysis

Neutron diffraction experiments were performed at the Advanced Neutron Diffractometer/Reflectometer (AND/R) at the National Institute of Standards and Technology (NIST) Center for Neutron Research (Gaithersburg, MD). The wavelength of the neutron beam was 5 Å. Each multilayer sample was hydrated using H_2O mixed with 0%, 20% and 50% D_2O. RH of 76% was achieved using a saturated NaCl solution, as previously described (Hristova and White 1998; Han et al. 2008). The solution was placed next to the sample in a sealed aluminum container, and diffraction pattern changes were recorded during sample equilibration. Typically, 6–7 h were needed for complete equilibration.

The diffraction intensity of each multilayer sample was measured during a Θ-2Θ scan using a He-3 gas-filled 25.4-mm-wide pencil detector (GE Reuter-Stokes, Twinsburg, OH). Initial data processing was performed using Reflred (http://www.ncnr.nist.gov/reflpak/reflred.html), a software written for AND/R. Further data processing, yielding the structure factors, was done with the commercially available package Origin (OriginLab, Northampton, MA).

The observed structure factors were calculated as

$$f(h) = \sqrt{I(h)A(h)\sin(2\Theta)} \quad (1)$$

where *I(h)* is the intensity of peak *h*, *A(h)* is the absorption correction and sin(2Θ) is the Lorentz factor. The absorption correction is given by (Worcester and Franks 1976)

$$A(h) = \frac{\sin\Theta}{2\mu t}\left[1 - \exp^{-2\mu t/\sin\Theta}\right] \quad (2)$$

where Θ is the Bragg angle, *t* is the sample thickness and μ is the linear absorption coefficient of the sample.

Experimental uncertainties in the structure factors were determined as described below and in Hristova et al. (1999) and Hristova and White (1998). Random errors in the experimental structure factors were minimized by placing the structure factors for each sample on a self-consistent arbitrary scale and linearizing them with D_2O concentration, as shown in Figs. 1 and 2 (Wiener and White 1991c; Hristova and White 1998). This linear relationship was used to find the "best" statistical estimates of the observed structure factors from parameters of the best-fit straight lines passing through the experimental structure factors (see further details in Wiener and White 1991c; Hristova and White 1998). The best structure factors calculated for

100% H_2O were used for structural characterization as described below.

Absolute Scaling: Overview

The absolute scattering length density $\rho^*(z)$ is the scattering length density per one lipid molecule, given by (Jacobs and White 1989)

$$\rho*(z) = \rho(z)S = \rho_0* + \frac{2}{d}\cdot\frac{1}{\bar{k}}\sum_{h=1}^{h_{obs}} f(h)\cos\left(\frac{2\pi hz}{d}\right) \qquad (3)$$

where ρ_0* is the average scattering length density of the unit cell, $f(h)$ is the measured structure factor on an arbitrary scale, $\bar{k}$ is the instrumental constant, d is the Bragg spacing and h_{obs} is the highest observed diffraction order. $F(h) = f(h)/\bar{k}$ are the absolute structure factors, which are determined solely by the structure and the scattering of the unit cell (Wiener and White 1991c; Hristova and White 1998).

As discussed previously (Han et al. 2006), the instrumental constant $\bar{k}$ and the absolute structure factors $F(h) = f(h)/\bar{k}$ can be determined for two samples, with unit cells which are identical except for a few atoms that have large differences in scattering lengths (i.e., isomorphous unit cells). Here, the absolute structure factors were determined by comparing scattering length density profiles for POPC bilayers, with and without 4 mole% FGFR3 TM domain, in the presence and absence of 20% $POPC^D$. Thus, the deuterium in the palmitoyl chain of $POPC^D$ served as a "label" that allowed us to both scale the data and determine the probability of finding the palmitoyl chain (i.e., the distribution of the palmitoyl chain) across the bilayer.

Two methods can be used to scale the structure factors: the "real space scaling method" (Wiener and White 1991c) and the "reciprocal space" scaling method (Hristova and White 1998). The reciprocal space method works for label distributions which are gaussian. Since we cannot expect that the acyl chain distribution is described by a single gaussian (in fact, it is known that the DOPC CH_2 distribution is described by three gaussians at 66% RH (Wiener and White 1992)), the real space scaling method was adopted in this study. This method, first used by Wiener and White (1991c) to scale DOPC profiles at 66% RH, is based on the assumption that the profiles of the isomorphous unit cells are identical in a region that is never visited by the labeled moiety. Two points within this region, z_1 and z_2, are used in equations describing the profile overlap to determine the instrumental constants for

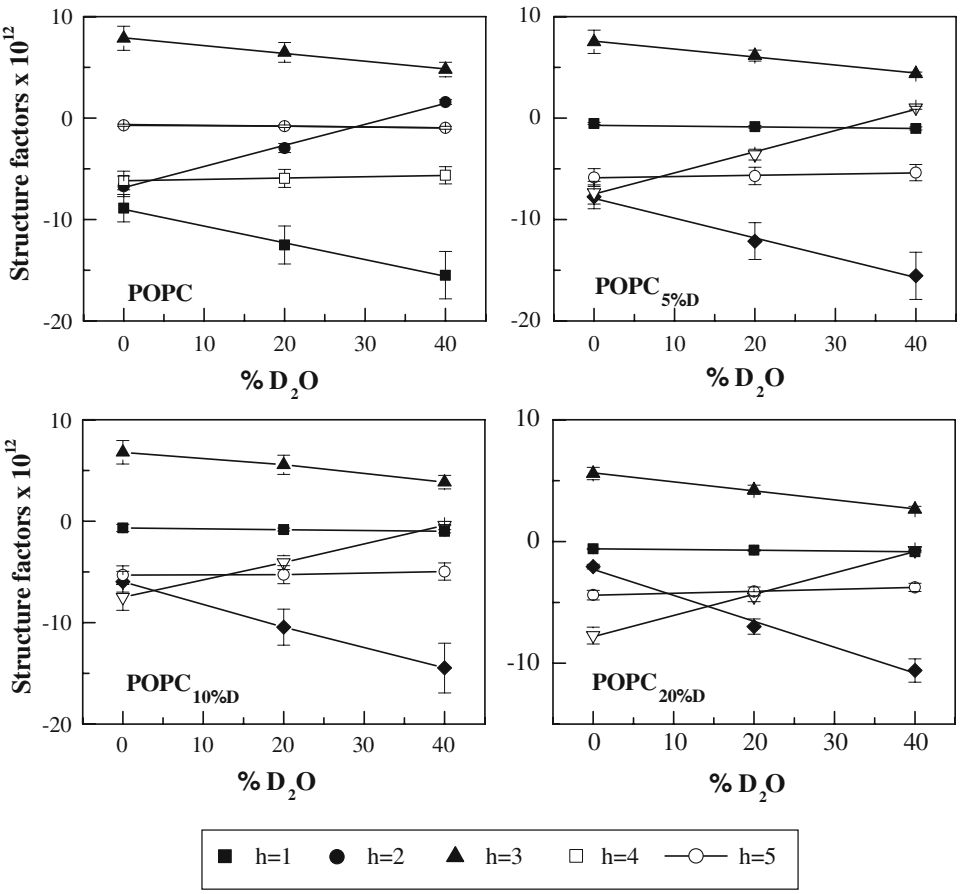

Fig. 1 Absolute structure factors of POPC bilayers with 0%, 5%, 10% and 20% $POPC^D$, as a function of D_2O mole%. The experimental uncertainties were calculated as described previously (Hristova et al. 2001). *Solid lines* are the linear fit to the data. For a given D_2O mole%, a point on the line is the best estimate of the structure factor

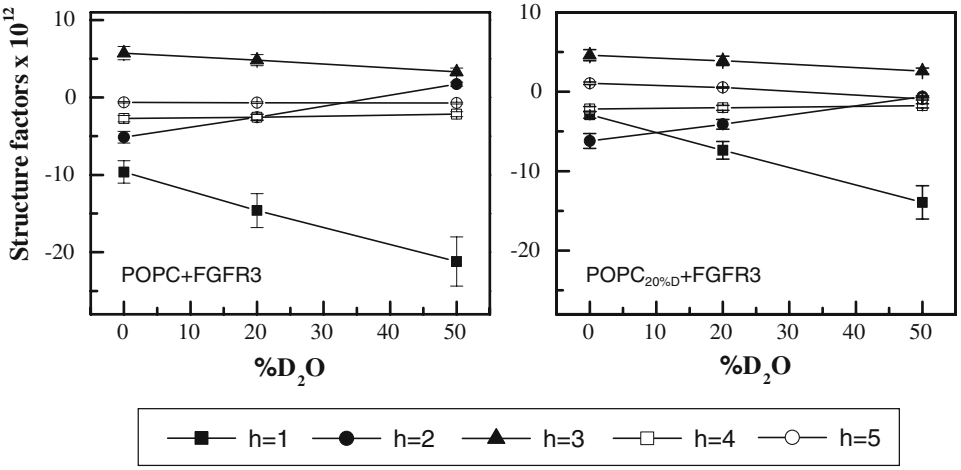

Fig. 2 Absolute structure factors of POPC bilayers with 4 mole% FGFR3 TM domain in the absence (left) and presence (right) of 20% $POPC^D$ as a function of D_2O mole%

the two isomorphous samples. Since the "label" used in this study was the deuterated palmitoyl chain, z_1 and z_2 were chosen close to the edge of the unit cell, in the water region of the bilayer. Thus, for the scaling it was assumed that the HC distribution does not reach the edge of the unit cell. This assumption is validated in "Results."

Because the two profiles are assumed to overlap at z_1 and z_2, the following two equations hold (Wiener and White 1991c):

$$\left(\frac{2}{d}k_A\right)\sum_{h=1}^{h_{obs}} f_A(h)\cos(2\pi h z_1/d) - \left(\frac{2}{d}k_B\right)\sum_{h=1}^{h_{obs}} f_B(h)\cos(2\pi h z_1/d) = \Delta\rho* \quad (4)$$

$$\left(\frac{2}{d}k_A\right)\sum_{h=1}^{h_{obs}} f_A(h)\cos(2\pi h z_2/d) - \left(\frac{2}{d}k_B\right)\sum_{h=1}^{h_{obs}} f_B(h)\cos(2\pi h z_2/d) = \Delta\rho* \quad (5)$$

In these equations, f_A and f_B are the structure factors for bilayers with different concentrations of $POPC^D$ and k_A and k_B are the corresponding scale factors. The parameter $\Delta\rho*$ is the scattering contrast introduced by the deuterated $POPC^D$ chain. The instrumental constants k_A and k_B are the unknowns, which are determined from Eqs. 4 and 5.

Protocol for Absolute Scaling and for Calculation of HC Thickness

The absolute scaling protocol uses the deuterium of the palmitoyl chain in $POPC^D$ as the "scaling label" and gives directly the transbilayer distribution of deuterated chain in POPC/$POPC^D$ bilayers. This protocol consists of four steps:

1. Neutron diffraction data are collected for POPC multilayers with various concentrations of $POPC^D$ (0%, 5%, 10%, 20%). The structure factors are calculated from the diffraction intensities using Eq. 1.
2. The structure factors are placed on the absolute scale using the real space protocol overviewed above. Pairs of profiles corresponding to different $POPC^D$ concentrations are scaled using Eqs. 4 and 5. The values of z_1 and z_2 are chosen as 25 and 26 Å from the bilayer center, close to the edge of the unit cell.
3. The difference between the absolute profiles obtained in step 2 is calculated. The difference profiles report the transbilayer distribution of the palmitoyl chain in the bilayer.
4. The width of the HC distribution is calculated as the width of the difference profiles at 1/e of the maximum amplitude (see Fig. 4).

Error Analysis

The absolute structure factor uncertainties depend on the uncertainties in the experimental structure factors, $\sigma(h)$, and on the error associated with calculating the scale factors, k. The experimental uncertainties, $\sigma(h)$, are determined from the square roots of the integrated peak areas and the background below the peaks, as described previously (Hristova et al. 1999; Hristova and White 1998).

The error in k can be determined based on the uncertainties, $\sigma(h)$, using the Monte Carlo method of Wiener and White (1992) (we refer to this as "method I"). Noise on the order of $\sigma(h)$ is added to the structure factors, $f(h)$, to create sets of mock structure factors, $f(h)^j$. Then, the scaling procedure (as described above) is carried out to obtain different estimates of the scale factor, k_j, and mock

absolute structure factors are calculated as $F(h)^j = k_j f(h)^j$. Their standard deviation provides one estimate of the absolute structure factor uncertainties.

Alternatively, uncertainties can be calculated if structure factors *f(h)* are available for more than two $POPC^D$ concentrations, as in the case here (we refer to this as "method II"). In this case, multiple instrumental constants, k_l, can be obtained for a single set of experimental structure factors, *f(h)*. As shown in Fig. 3, three instrumental constants, k_l, can be obtained for bilayers composed of 80% POPC and 20% $POPC^D$ by comparing this profile with profiles of POPC bilayers with 0%, 5% and 10% $POPC^D$. As a result, three estimates of the absolute structure factors, $F(h)^l = k_l f(h)$, can be obtained and their standard deviation is also a measure of the absolute structure factor uncertainties.

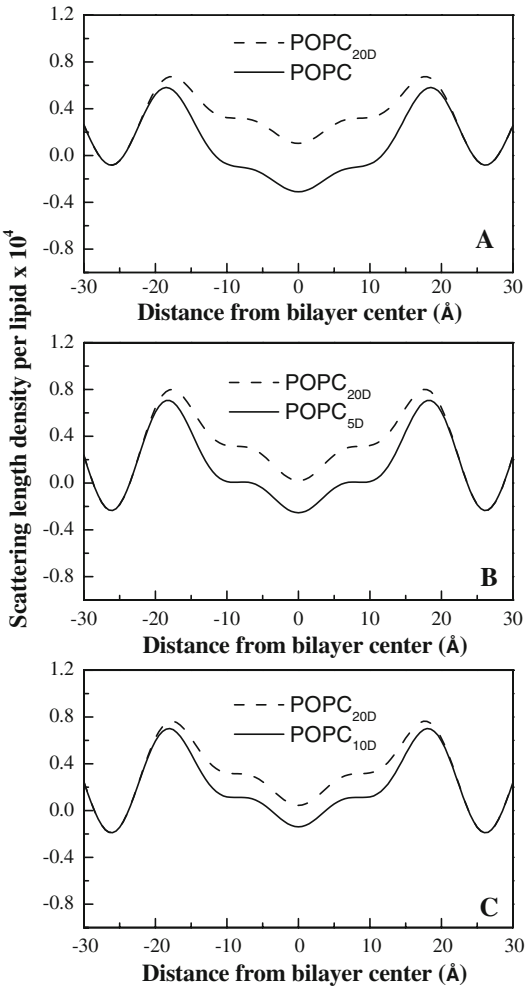

Fig. 3 Absolute scattering length density profiles for *POPC* bilayers with various $POPC^D$ concentrations: **a** 0% and 20% $POPC^D$, **b** 5% and 20% $POPC^D$, **c** 10% and 20% $POPC^D$. The obvious difference between each pair of profiles is due to the isomorphous replacement of 31 hydrogens with 31 deuterons in the palmitoyl chain of $POPC^D$, giving the palmitoyl chain distribution across the bilayer

Absolute structure factor uncertainties, calculated using methods I and II, were very similar.

Results

Direct Views of the POPC HC Distribution

To determine the HC transbilayer distribution in POPC bilayers, multilayers containing different concentrations of POPC and $POPC^D$ (with the palmitoyl chain deuterated) were prepared and analyzed as described in "Materials and Methods." Neutron diffraction experiments were carried out at the AND/R at NIST, and structure factors were calculated using Eq. 1. Absolute scattering length density profiles were calculated using Eq. 3. Structure factors and scattering length density profiles were placed on the absolute scale as described in "Materials and Methods," by choosing z_1 and z_2 as 25 and 26 Å from the bilayer center, close to the edge of the unit cell. Figures 1 and 2 show the plots of the absolute structure factors as a function of D_2O content, and Table 1 reports the "best" absolute structure factors for 100% H_2O. Figure 3 compares the absolute scattering length density profiles for POPC bilayers with 0 mole%, 5 mole%, 10 mole% and 20 mole% $POPC^D$. The difference between the profiles is due to the substitution of a fraction of POPC with $POPC^D$ (i.e., the isomorphous replacement of 31 hydrogens with 31 deuterons in the palmitoyl chain). Thus, the difference between the profiles, shown in Fig. 4, gives the transbilayer distribution of the palmitoyl chain. The amplitudes of the three difference profiles in Fig. 4, which reflect the scattering difference

Table 1 The "best" absolute structure factors and their experimental uncertainties for POPC multilayers with 0%, 5%, 10% and 20% $POPC^D$

h[a]	0% $POPC^D$	5% $POPC^D$	10% $POPC^D$	20% $POPC^D$
1	−8.99 ± 1.35	−7.91 ± 1.18	−6.03 ± 1.02	−2.24 ± 0.17
2	−6.85 ± 1.02	−7.50 ± 1.12	−7.54 ± 1.28	−7.70 ± 0.62
3	7.91 ± 1.19	7.59 ± 1.14	6.87 ± 1.16	5.54 ± 0.44
4	−6.17 ± 0.92	−5.89 ± 0.88	−5.34 ± 0.90	−4.33 ± 0.35
5	−0.64 ± 0.10	−0.72 ± 0.11	−0.66 ± 0.11	−0.59 ± 0.05
d (Å)[b]	52.4 ± 0.3	52.7 ± 0.3	52.3 ± 0.3	52.3 ± 0.3

Structure factors were calculated as described in "Materials and Methods" by comparing the scattering profiles of multiple pairs of samples with different concentrations of $POPC^D$. The reported values are the average of three independent calculations of the absolute structure factors along with the standard deviation. For example, three scale factors were obtained for POPC bilayers by comparing the pure POPC profile with profiles in the presence of 5%, 10% and 20% $POPC^D$

[a] Diffraction order

[b] Bragg spacing

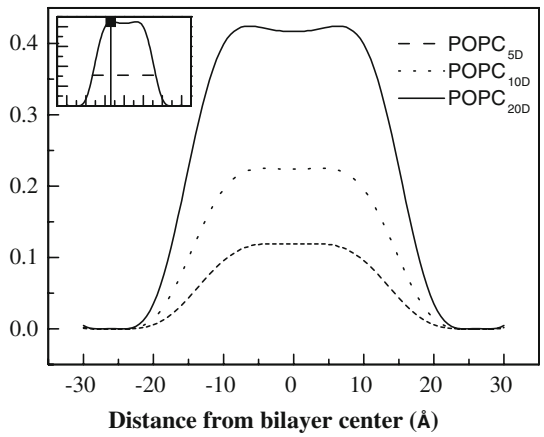

Fig. 4 Difference profiles, obtained via direct subtraction between the pairs of profiles shown in Fig. 3. These difference profiles report the palmitoyl chain distribution of POPC. The HC width is defined as the width at 1/e of the maximal amplitude of the difference profile (*inset*)

due to the addition of 5%, 10% and 20% $POPC^D$, scale with the difference in $POPC^D$ concentration.

The widths of the difference profiles shown in Fig. 4 were calculated as the widths at 1/e of the maximum amplitude of the profiles (see inset). These widths were obtained by comparing pairs of POPC profiles in the presence of different $POPC^D$ concentrations. As seen in Table 3, the six independent calculations of the HC width of POPC fall within ±2 Å around the average value of 33 Å.

The scaling procedure presented in "Materials and Methods" is based on the assumption that the edge of the unit cell is not visited by the palmitic methylene moieties of POPC. All the results shown are for $z_1 = 25$ Å and $z_2 = 26$ Å from the bilayer center. However, we also varied these values between 26.2 and 22.0 Å and obtained very similar results (instrumental constants within 5%, data not shown). Thus, the results of the scaling are not sensitive to the choice of z_1 and z_2 within 4 Å from the edge of the unit cell. Furthermore, the profiles virtually overlap (i.e., the difference profiles are practically zero) within 7 Å from the edge of the unit cell (see Fig. 4, not all results shown). These results demonstrate the validity of the scaling procedure given in "Materials and Methods" as well as the validity of the underlying assumption that the HC distribution vanishes close to the edge of the unit cell.

Table 2 The "best" absolute structure factors of POPC multilayers with 4 mole% FGFR3 TM domain in the absence and presence of 20% $POPC^D$

h[a]	POPC + FGFR3[c]	POPC + FGFR3	20% $POPC^D$ + FGFR3
1	−10.13 ± 1.50	−10.43 ± 1.53	−3.02 ± 0.45
2	−5.40 ± 0.81	−5.59 ± 0.82	−6.36 ± 0.95
3	6.03 ± 0.91	6.17 ± 0.93	4.70 ± 0.71
4	−2.87 ± 0.43	−2.95 ± 0.45	−2.22 ± 0.27
5	−0.66 ± 0.61	−0.67 ± 0.62	0 ± 0.35
d (Å)[b]	49.5 ± 0.3	49.5 ± 0.3	49.3 ± 0.3

Structure factors and their experimental uncertainties were calculated using the protocol described in "Materials and Methods"

[a] Diffraction order

[b] Bragg spacing

[c] Structure factors scaled in a previous study (Hristova et al. 2001) using the reciprocal space method and deuterated amino acids as the "scaling label." The new scaling method gives similar results

The HC Distribution in the Presence of FGFR3 TM Domain

Next, we calculated the HC distribution along the bilayer normal in the presence of FGFR3 TM domain using the scaling protocol given in "Materials and Methods."

Two multilayer samples were characterized: (1) 96 mole% POPC + 4 mole% FGFR3 TM domain and (2) 96 mole% lipid (80 mole% POPC and 20 mole% $POPC^D$) + 4 mole% FGFR3 TM domain. Structure factors (Table 2) and profiles (Fig. 5) were placed on the absolute scale as described in "Materials and Methods."

In our previous work (Han et al. 2006), structure factors for POPC multilayers with 4 mole% FGFR3 TM domain were scaled using specifically deuterated amino acids and

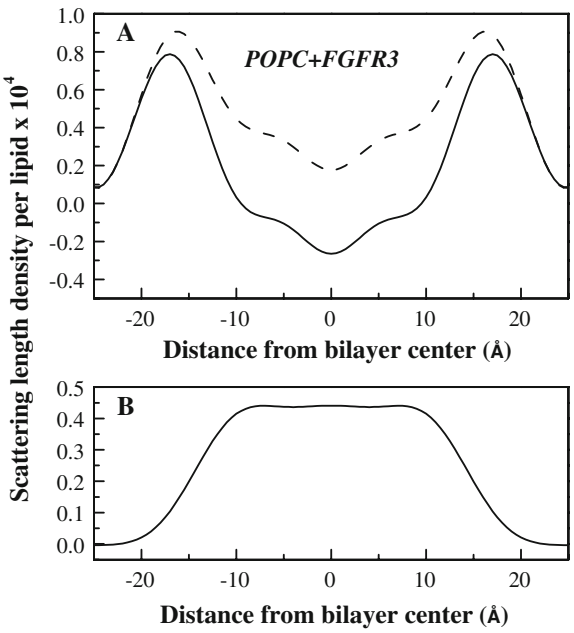

Fig. 5 **a** Absolute scattering length density profiles for *POPC* bilayers with 4 mole% FGFR3 TM domain in the presence (*dashed line*) and absence (*solid line*) of 20 mole% $POPC^D$. **b** Difference profile showing the palmitoyl chain distribution in the presence of 4 mole% FGFR3 TM domain

Table 3 HC widths obtained by comparing pairs of profiles of POPC bilayers with either 0 mole%, 5 mole%, 10 mole% or 20 mole% $POPC^D$

Width (Å)	0–5%	0–10%	0–20%	5–10%	5–20%	10–20%	Average
POPC	30.0 ± 1.7	31.6 ± 2.2	33.2 ± 2.0	34.6 ± 2.1	34.8 ± 1.8	34.8 ± 1.8	33 ± 2
POPC + FGFR3			31.4 ± 1.9				

HC width is defined as the width at 1/e of the hydrocarbon core profile maximum. Also shown is the width in the presence of 4 mole% FGFR3 TM domain, which falls within the range observed for pure lipid bilayers. Thus, no change in HC width can be detected upon peptide incorporation

the reciprocal space scaling method (results shown in Table 2, column 1). Here, the structure factors were scaled using the deuterated palmitoyl chain as the "label" and the real space scaling method (Table 2, columns 2 and 3). Comparison between columns 1 and 2 in Table 2 demonstrates that the two scaling methods give very similar results, further confirming that the scaling procedure described in "Materials and Methods" is robust. This procedure also gives directly the distribution of the palmitoyl chain of $POPC^D$.

Figure 5 shows the absolute neutron scattering length density profiles for *POPC* bilayers with 4 mole% FGFR3 TM domain in the presence and absence of 20 mole% $POPC^D$. The difference profile, obtained by simple subtraction, shows the palmitoyl chain distribution. The 1/e width of the palmitoyl chain distribution, giving the HC thickness, is 31.4 Å (see Table 3). This value is similar to the 33 ± 2 Å value obtained in the absence of the peptide.

Discussion

Hydrogen–deuterium exchange combined with neutron scattering is a powerful tool in structural biology (Zaccai 2000; Trewhella et al. 1998). This exchange does not introduce structural perturbations and allows precise determination of the spatial distribution of the deuterium label. This technique is used with both small angle neutron scattering (SANS) (Petoukhov and Svergun 2007), to gain information about macromolecular structure and assembly in solution (Pencer et al. 2005), and with diffraction/reflectivity, to elucidate structures within multilayers (Meuse et al. 1998; Krueger et al. 2001). In bilayers or lipid multilayers, specific deuteration of amino acids can provide valuable insights into protein disposition in the bilayer (Bradshaw et al. 2000a, 2000b; Dante et al. 2002; Hauss et al. 2005). Specific deuteration of chosen amino acids is easy to implement if the peptides are produced via solid-phase peptide synthesis, where any fluorenylmethoxycarbonyl (Fmoc) amino acid can be substituted with its deuterated version during production. In such experiments, the transbilayer distribution of a deuterated amino acid is given by a gaussian distribution and the center of the gaussain points to the position of the amino acid within the bilayer thickness. Work from several laboratories has revealed that this approach to structural determination is feasible (Bradshaw et al. 2000a, 2000b; Dante et al. 2002; Hauss et al. 2005) and can be successfully used to test predictions for membrane-embedded segments based on hydrophobicity scales (Han et al. 2006) and to evaluate various contributions to protein folding in membrane environments (Han et al. 2008).

Since membrane protein folding occurs within the context of the native bilayer, structural studies of bilayers with and without proteins have proven invaluable in deciphering the physical principles behind membrane protein stability (White et al. 1998, 2001; Li and Hristova, 2006). Yet, complete structures of bilayers are difficult to obtain. An obvious question that arises is whether an approach that is similar to using deuterated amino acids, i.e., using specifically deuterated lipids, would be a useful tool to study bilayer structures. There are commercially available lipids that either are fully deuterated or have deuterated acyl chains. Such lipids are widely used in nuclear magnetic resonance studies but are not yet fully utilized in neutron diffraction studies. Here, we used POPC lipids with one deuterated acyl chain to obtain the distribution of the HC and, ultimately, the thickness of the HC at 76% RH. The data can be compared to previous measurements of fully hydrated POPC bilayers, such as the ones of Kucerka et al (2006). These measurements, based on less direct structural characterization of the HC of POPC, have yielded a thickness value of 27.1 Å. The HC thickness is known to decrease when hydration is increased, by at least 3 Å (Hristova and White 1998); thus, the measurements at low and high hydration appear consistent with each other. Furthermore, our result for the POPC HC thickness at 76% RH is similar to the HC thickness of DOPC bilayers at 66% RH, 32 Å (Wiener and White 1992), obtained within the context of the complete DOPC structure.

Here, we used deuterated lipids to monitor the HC in the presence of a TM peptide corresponding to the TM domain of a human receptor tyrosine kinase, the TM domain of FGFR3; and we saw no change in the HC thickness upon peptide incorporation (Table 3). The peptide disposition inside the bilayer has been previously characterized using oriented circular dichroism and neutron diffraction (Han et al. 2006). It is highly helical and transmembrane, and the

helix tilt with respect to the normal bilayer does not exceed 20 degrees. The hydrophobic length of the helix can be calculated as the number of consecutive hydrophobic amino acids in the sequence (24) times the rise per residue in a helix (1.5 Å), i.e., 24×1.5 Å $= 36$ Å, similar to the measured value of 33 ± 2 Å. To the best of our knowledge, this is the first such study of the effect of a human TM sequence on bilayer structure, which underscores the need for simple structural methods that are applicable for fluid bilayer environments. We believe that the simple experimental approach presented here will aid future structural studies of proteins incorporated into lipid bilayers.

Acknowledgement We thank Drs. M. Mihailescu and D. Worcester for their help with neutron data collection and processing and for useful discussions. This work was supported by National Institutes of Health (NIH) grant GM068619 (to K. H.). We acknowledge the support of the National Institute of Standards and Technology, U.S. Department of Commerce, and the Cold Neutrons for Biology and Technology (CNBT) program funded by the NIH under grant RR14812 and the Regents of the University of California, for providing the neutron research facilities used in this work.

References

Bradshaw JP, Darkes MJM, Harroun TA, Katsaras J, Epand RM (2000a) Oblique membrane insertion of viral fusion peptide probed by neutron diffraction. Biochemistry 39:6581–6585

Bradshaw JP, Darkes MJM, Katsaras J, Epand RM (2000b) Neutron diffraction studies of viral fusion peptides. Physica B 276:495–498

Dante S, Hauss T, Dencher NA (2002) Beta-amyloid 25 to 35 is intercalated in anionic and zwitterionic lipid membranes to different extents. Biophys J 83:2610–2616

Gandhavadi M, Allende D, Vidal A, Simon SA, McIntosh TJ (2002) Structure, composition, and peptide binding properties of detergent soluble bilayers and detergent resistant rafts. Biophys J 82:1469–1482

Han X, Mihailescu M, Hristova K (2006) Neutron diffraction studies of fluid bilayers with transmembrane proteins: structural consequences of the achondroplasia mutation. Biophys J 91:3736–3747

Han X, Hristova K, Wimley WC (2008) Protein folding in membranes: insights from neutron diffraction studies of a membrane beta-sheet oligomer. Biophys J 94:492–505

Harroun TA, Heller WT, Weiss TM, Yang L, Huang HW (1999) Experimental evidence for hydrophobic matching and membrane-mediated interactions in lipid bilayers containing gramicidin. Biophys J 76:937–945

Hauss T, Dante S, Haines TH, Dencher NA (2005) Localization of coenzyme Q_{10} in the center of a deuterated lipid membrane by neutron diffraction. Biochim Biophys Acta 1710:57–62

Heller WT, Waring AJ, Lehrer RI, Harroun TA, Weiss TM, Yang L, Huang HW (2000) Membrane thinning effect of the β-sheet antimicrobial protegrin. Biochemistry 39:139–145

Hristova K, White SH (1998) Determination of the hydrocarbon core structure of fluid dioleoylphosphocholine (DOPC) bilayers by X-ray diffraction using specific bromination of the double-bonds: effect of hydration. Biophys J 74:2419–2433

Hristova K, Wimley WC, Mishra VK, Anantharamaiah GM, Segrest JP, White SH (1999) An amphipathic α-helix at a membrane interface: a structural study using a novel X-ray diffraction method. J Mol Biol 290:99–117

Hristova K, Dempsey CE, White SH (2001) Structure, location, and lipid perturbations of melittin at the membrane interface. Biophys J 80:801–811

Iwamoto T, You M, Li E, Spangler J, Tomich JM, Hristova K (2005) Synthesis and initial characterization of FGFR3 transmembrane domain: consequences of sequence modifications. Biochim Biophys Acta 1668:240–247

Jacobs RE, White SH (1989) The nature of the hydrophobic binding of small peptides at the bilayer interface: implications for the insertion of transbilayer helices. Biochemistry 28:3421–3437

Katsaras J, Stinson RH, Davis JH, Kendall EJ (1991) Location of two antioxidants in oriented model membranes—small-angle X-ray diffraction study. Biophys J 59:645–653

Krueger S, Meuse CW, Majkrzak CF, Dura JA, Berk NF, Tarek M, Plant AL (2001) Investigation of hybrid bilayer membranes with neutron reflectometry: probing the interactions of melittin. Langmuir 17:511–521

Kucerka N, Tristram-Nagle S, Nagle JF (2006) Structure of fully hydrated fluid phase lipid bilayers with monounsaturated chains. J Membr Biol 208:193–202

Li E, Hristova K (2004) Imaging FRET measurements of transmembrane helix interactions in lipid bilayers on a solid support. Langmuir 20:9053–9060

Li E, Hristova K (2006) Role of receptor tyrosine kinase transmembrane domains in cell signaling and human pathologies. Biochemistry 45:6241–6251

MacKenzie KR (2006) Folding and stability of alpha-helical integral membrane proteins. Chem Rev 106:1931–1977

Meuse CW, Krueger S, Majkrzak CF, Dura JA, Fu J, Connor JT, Plant AL (1998) Hybrid bilayer membranes in air and water: infrared spectroscopy and neutron reflectivity studies. Biophys J 74:1388–1398

Nagle JF, Tristram-Nagle S (2001) Structure of lipid bilayers. Biochim Biophys Acta 1469:159–195

Nagle JF, Wiener MC (1988) Structure of fully hydrated bilayer dispersions. Biochim Biophys Acta 942:1–10

Pencer J, Krueger S, Epand R, Katsaras J (2005) Detection of submicron-sized domains or so-called "rafts" in membranes by small-angle neutron scattering. Biophys J 88:76A

Petoukhov MV, Svergun DI (2007) Analysis of X-ray and neutron scattering from biomacromolecular solutions. Curr Opin Struct Biol 17:562–571

Trewhella J, Gallagher SC, Krueger JK, Zhao J (1998) Neutron and X-ray solution scattering provide insights into biomolecular structure and function. Sci Prog 81:101–122

White SH, Wimley WC, Ladokhin AS, Hristova K (1998) Protein folding in membranes: pondering the nature of the bilayer milieu. Biol Skr Dan Selsk 49:91–98

White SH, Wimley WC (1999) Membrane protein folding and stability: physical principles. Annu Rev Biophys Biomol Struct 28:319–365

White SH, Ladokhin AS, Jayasinghe S, Hristova K (2001) How membranes shape protein structure. J Biol Chem 276:32395–32398

Wiener MC, Suter RM, Nagle JF (1989) Structure of the fully hydrated gel phase of dipalmitoylphosphatidylcholine. Biophys J 55:315–325

Wiener MC, King GI, White SH (1991) Structure of a fluid dioleoylphosphatidylcholine bilayer determined by joint refinement of X-ray and neutron diffraction data. I. Scaling of neutron data and the distribution of double-bonds and water. Biophys J 60:568–576

Wiener MC, White SH (1991a) Fluid bilayer structure determination by the combined use of X-ray and neutron diffraction. I. Fluid

bilayer models and the limits of resolution. Biophys J 59:162–173

Wiener MC, White SH (1991b) Fluid bilayer structure determination by the combined use of X-ray and neutron diffraction. II. "Composition-space" refinement method. Biophys J 59:174–185

Wiener MC, White SH (1991c) Transbilayer distribution of bromine in fluid bilayers containing a specifically brominated analog of dioleoylphosphatidylcholine. Biochemistry 30:6997–7008

Wiener MC, White SH (1992) Structure of a fluid dioleoylphosphatidylcholine bilayer determined by joint refinement of X-ray and neutron diffraction data. III. Complete structure. Biophys J 61:434–447

Worcester DL, Franks NP (1976) Structural analysis of hydrated egg lecithin and cholesterol bilayers. II. Neutron diffraction. J Mol Biol 100:359–378

You M, Li E, Wimley WC, Hristova K (2005) FRET in liposomes: measurements of TM helix dimerization in the native bilayer environment. Anal Biochem 340:154–164

Zaccai G (2000) Moist and soft, dry and stiff: a review of neutron experiments on hydration–dynamics–activity relations in the purple membrane of *Halobacterium salinarum*. Biophys Chem 86:249–257